Materials Research Letters

ISSN: (Print) 2166-3831 (Online) Journal homepage: https://www.tandfonline.com/loi/tmrl20

Toward edges-rich MoS_2 layers via chemical liquid exfoliation triggering distinctive magnetism

Guanhui Gao, Chi Chen, Xiaobin Xie, Yantao Su, Shendong Kang, Guichi Zhu, Duyang Gao, Achim Trampert & Lintao Cai

To cite this article: Guanhui Gao, Chi Chen, Xiaobin Xie, Yantao Su, Shendong Kang, Guichi Zhu, Duyang Gao, Achim Trampert & Lintao Cai (2017) Toward edges-rich MoS_2 layers via chemical liquid exfoliation triggering distinctive magnetism, Materials Research Letters, 5:4, 267-275, DOI: 10.1080/21663831.2016.1256915

To link to this article: https://doi.org/10.1080/21663831.2016.1256915

MATER. RES. LETT., 2017
VOL. 5, NO. 4, 267–275
https://doi.org/10.1080/21663831.2016.1256915

MATERIALS RESEARCH LETTERS
Taylor & Francis
Taylor & Francis Group

ORIGINAL REPORT

Toward edges-rich MoS_2 layers via chemical liquid exfoliation triggering distinctive magnetism

Guanhui Gao[a,b], Chi Chen[c], Xiaobin Xie[d], Yantao Su[e], Shendong Kang[a], Guichi Zhu[f], Duyang Gao[g], Achim Trampert[b] and Lintao Cai[a]

[a]Guangdong Key Laboratory of Nanomedicine, Shenzhen Institutes of Advanced Technology, Chinese Academy of Science, Shenzhen, People's Republic of China; [b]Paul-Drude-Institut für Festkörperelektronik, Berlin, Germany; [c]NanoBioPhotonics, Center for Nanoscience and Nanotechnology, Institute for Integrative Biology of the Cell, Université Paris-Sud, Orsay, France; [d]Debye Institute for Nanomaterials Science, Utrecht University, Utrecht, The Netherlands; [e]School of Advanced Materials, Peking University Shenzhen Graduate School, Peking University, Shenzhen, People's Republic of China; [f]Laboratory of Biosensors and Nanomachines, Department of Chemistry, University of Montreal, Montreal, Quebec, Canada; [g]Bioimaging Core, Faculty of Health Sciences, University of Macau, Taipa, People's Republic of China

ABSTRACT

The magnetic function of layered molybdenum disulfide (MoS_2) has been investigated via simulation, but few reliable experimental results have been explored. Herein, we developed edges-rich structural MoS_2 nanosheets via liquid phase exfoliation approach, triggering exceptional ferromagnetism. The magnetic measurements revealed the clear ferromagnetic property of layered MoS_2, compared to the pristine MoS_2 in bulk exhibiting diamagnetism. The existence of ferromagnetism mostly was attributed to the presence of grain boundaries with abundant irregular edges confirmed by the transmission electron microscopy, magnetic force microscopy and X-ray photoelectron spectroscopy, which experimentally provided reliable evidences on irregular edges-rich states engineering ferromagnetism to clarify theoretical calculation.

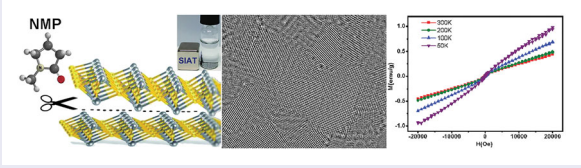

IMPACT STATEMENT

- Edges-rich MoS_2 layers are achieved via chemical liquid approach.
- The abundant edges MoS_2 nanosheets demonstrate highly superior magnetic property, which provides reliable evidences to identify irregular edge states engineering ferromagnetism experimentally.

ARTICLE HISTORY
Received 24 May 2016

KEYWORDS
Edges-rich MoS_2; exfoliation; magnetic property; grain boundaries

Introduction

Intense interest has been paid on the atomically thin two-dimensional transition metal dichalcogenides (TMDs), triggering distinctive properties (electronics, optoelectronics, and magnetism), which can dramatically differ from those of the corresponding bulk crystals [1–8]. Representatively, the advances on the edge-dependent of molybdenum disulfide (MoS_2) have rendered in applications of electric devices, photovoltaic cell, photo-catalyst and semiconductors [9–19]. Very recently, the strain effects of low-dimensional materials were carried out dramatically to understand their electric/magnetic properties [20,21]. Particularly, the magnetic function of MoS_2 nanosheets was evaluated and tuned and by applying the strain effects via the first-principle simulations [22,23].

According to the directions of termination, there existed two kinds of edges: armchair and zigzag states. Pan H. et al. proposed the essence of the ferromagnetism in MoS_2 with zigzag edges. It reported that the magnetic properties of MoS_2 nanosheets can be evaluated by simulating the energy difference between the nonmagnetic

CONTACT Lintao Cai lt.cai@siat.ac.cn Bioimaging Core, Guangdong Key Laboratory of Nanomedicine, CAS Key Laboratory of Health Informatics, Shenzhen Institutes of Advanced Technology, Chinese Academy of Science, Shenzhen 518055, People's Republic of China

Supplemental data for this article can be accessed at doi:10.1080/21663831.2016.1256915

and magnetic states [24,25]. The energies of nonmagnetic states in armchair edges were equal to those of magnetic states, exhibiting nonmagnetic activity. Comparably, the energies of nonmagnetic states in zigzag edge structures were higher than those of magnetic states, demonstrating the typical magnetic property [26–29]. The calculations illustrated that the MoS_2 nanosheets with armchair edges were nonmagnetic while these of zigzag edges were magnetic.

Theoretically, it has been reported that zigzag-edged graphene nanosheets have localized electrons at edge carbon atoms [30–34]. And there was ongoing work by Chen et al. presenting the distinctive magnetism of graphene with irregular zigzag edges experimentally [35]. Comparably, Magnetic MoS_2 layers should be more suitable for spintronic potentials than graphene because ferromagnetic graphene can only be achieved by applying external electrical/magnetic field, thus the magnetic moments/states of zigzag MoS_2 would be higher/stronger than those of graphene nanosheets. Terrones calculated that the zigzag MoS_2 nano-ribbons exhibited extraordinary magnetic properties even if the ribbons were passivated with hydrogen atoms [25]. However, there have not been a few works that supported experimentally, but only Gao et al. mentioned the intrinsic ferromagnetism of MoS_2 nanosheets was related to the presence of edge spins [36]. Han et al. employed proton irradiation or annealing in the hydrogen condition to induce the ferromagnetic order from diamagnetic MoS_2 crystals, resulting in an promoted transport property [37].

Here, we explored single, double and multi-layered MoS_2 via chemical liquid approach by means of intensive sonication, harnessing to exfoliate or delaminate atomic nanosheets (Figure 1 and experimental section in details). Previously, we have demonstrated this approach to exfoliate hexagonal boron nitrite (h-BN) and layered graphene (G), creating artificially building blocks as stacked h-BN/G hybrids [38]. It allowed the confinement of electrons upon exfoliation leading to unprecedented magnetic and electrical properties. Particularly, the edge-dependent magnetism was superior to exhibit with the advances on the abundant edges MoS_2 nanosheets. Additionally, it can be scaled up the exfoliation process with high yield, expecting to explore more potential applications in electromagnetism devices, and pave the way for magnetic development of 2D MoS_2.

Experimental

Preparation of single-, double- and multi-layered MoS_2. MoS_2 powders were purchased from Sigma Aldrich; N-methyl-pyrrolidone (NMP) and isopropanol (IPA) solvents were purchased from Aldrich and used as supplied.

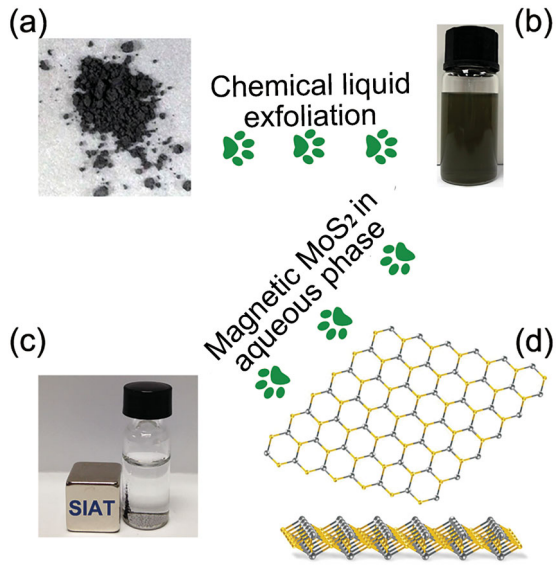

Figure 1. Schematic depiction of the exfoliated MoS_2 with magnetism via chemical liquid strategy. (a) Bulk MoS_2 powder with size around 1.0 μm. (b) A dispersion of exfoliated MoS_2 in IPA solution. (c) Layered MoS_2 nanosheets dispersed in water, demonstrating the ferromagnetism clearly. (d) Atomic layer MoS_2 arrangement of S and Mo atoms model.

All other reagents and solvents were of analytical grade. Pristine MoS_2 powder dissolved in NMP solvent (initial concentration of 0.5 mg/ml) sonicating in a low power sonic bath (Fisherbrand FB15061, 750 W) for 4 h. Then the above mixture was transferred to a higher power sonicator (Coleparmer 1200 W) and continually to be sonicated for 6 h. Finally, the mixture was centrifuged at 3000 rpm for 40 min, the supernatant was collected by pipette and filtered with filtration system. The above-filtered flakes of MoS_2 nanosheets were then dispersed into IPA uniformly, then dried at 60°C, finally, the exfoliated MoS_2 nano-layers containing single, double and multi-layered (less than 10 layers) were stored in vacuum to be investigated further characteristics. The obtained MoS_2 layers were dissolve into aqueous solution to evaluate their dispersity and magnetic separation by placing a magnet aside (Figure 1(c)).

Instrumentation

Transmission electron microscopy (TEM), high-resolution bright-field (HRTEM), high angle annular dark-field (HAADF) images and energy-dispersive X-ray spectroscopy (EDS) measurements were carried out with the field emission FEI-F30, operated at 200 kV. X-ray photoelectron spectroscopy spectra (XPS) data were taken by Thermo ESCALAB 250XI Multifunctional imaging electron spectrometer, which was equipped with

a Al Kα source. XPS data was analyzed with the MultiPak software. Raman spectroscopy was used to characterize the structure of the film at 514 nm laser excitation. Optical absorptance measurements (Shimadzu ultraviolet-3600) were performed using 1 cm quartz. X-ray diffraction (XRD) with Rigaku D/Max Ultima II Powder XRD configured with a vertical theta/theta goniometer, Cu Ka radiation, graphite monoichrometer, and scintillation counter. The hysteresis loop character was measured using the DH4516N Dynamic hysteresis and analyzed with Magnetic Data Analysis Solution (MDAS). The physical property measurement system (PPMS) was carried with the model P525 vibrating sample magnetometer (VSM). All samples were loaded into the typical nonmagnetic capsule supported by Quantum Design Company to investigate the VSM (please see the supporting information S1 for more detailed measurement). Magnetic force microscope (MFM) and atomic force microscope (AFM) measurements were conducted by the Dimension 3100, Veeco. The UV-vis absorbance spectrum was conducted with the PerkinElmer Lambda 750 absorption spectrophotometer. All above data was plotted and analyzed by using Origin-Pro 8 software.

Results and discussion

Individual and multi-layered MoS_2 nanosheets were observed via TEM and HRTEM as shown in Figure 2(a) and (b). The insight of edges-rich structural MoS_2 layers was obtained with scanning transmission electron microscopy (STEM) image (Figure 2(c)), indicating the hexagonal atomic arrangement, the insert in Figure

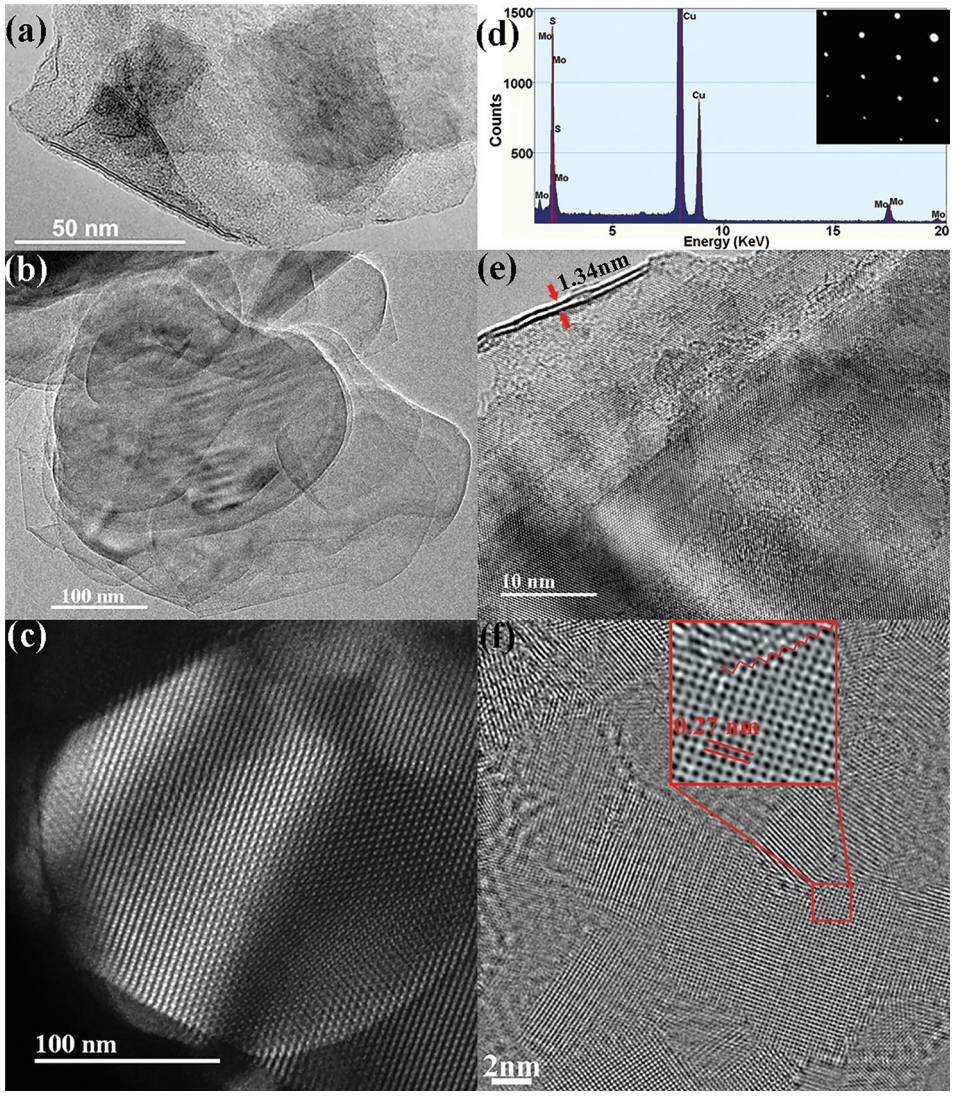

Figure 2. Morphology and lattice structure of edges-rich MoS_2 layers. (a) and (b) TEM images of the exfoliated MoS_2 layers. (c) HAADF image of single layer MoS_2 nanosheet. (d) EDS image of exfoliated MoS_2 layers, and insert was the SAED pattern. (e) and (f) High-resolution bright-field TEM images of single and double layers MoS_2. The region indicated by square was enlarged to show the edges and basal plane hexagonal structures.

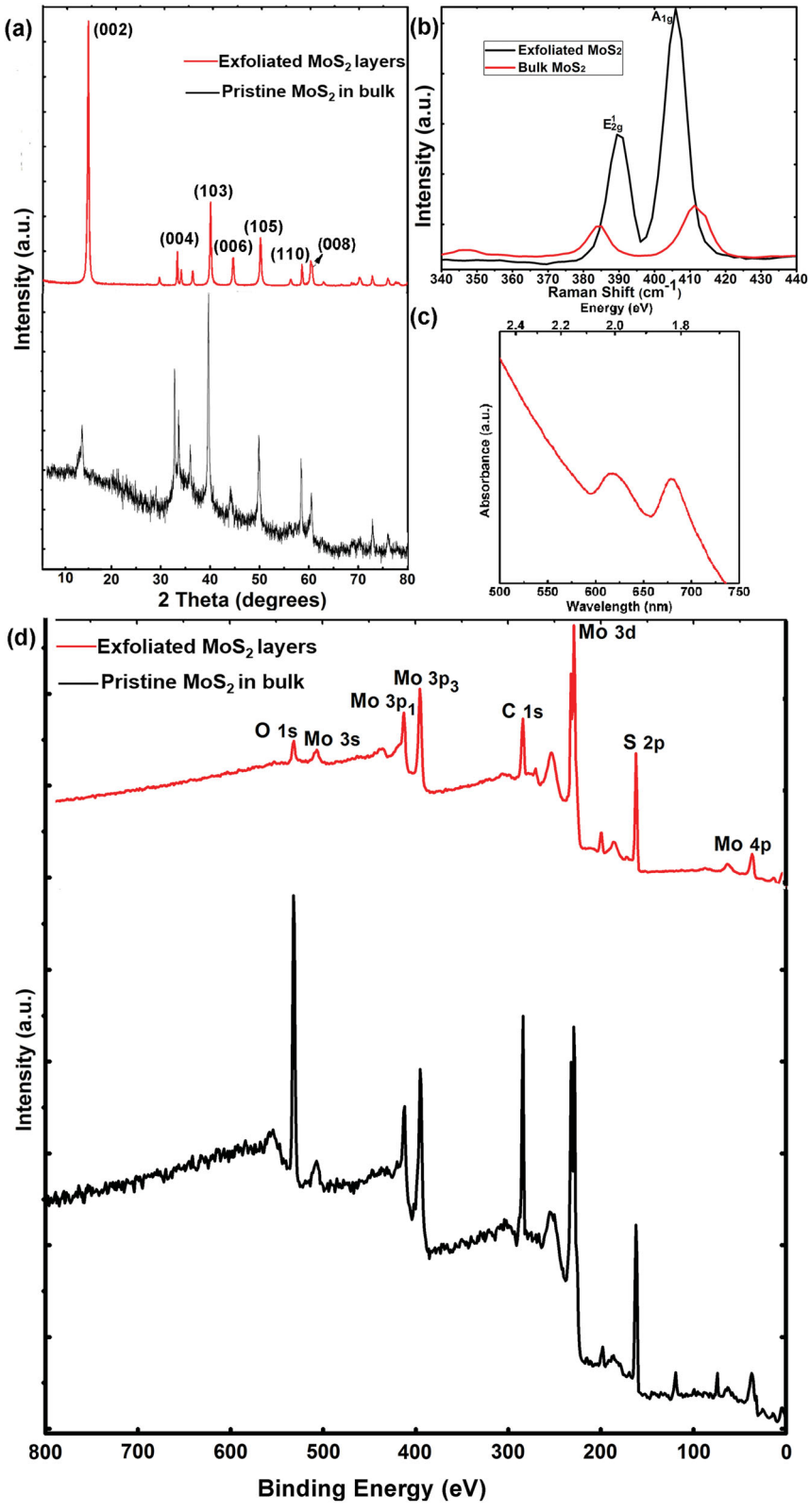

Figure 3. Evidence for exfoliated edges-rich MoS_2 structure. (a) XRD pattern taken on the exfoliated MoS_2 nanosheets and bulk MoS_2. (b) Raman spectra captured on the exfoliated MoS_2 and pristine MoS_2 in bulk. (c) UV-vis absorption spectrum of exfoliated MoS_2. (d) XPS spectrum of the exfoliated MoS_2 nanosheets and bulk MoS_2 for full scanning.

2(d) was selected area electron diffraction (SAED) pattern corresponding with the STEM measurement. It was essential to point out that there were single, double and multi-layered (less than 10 layers) existed in this typical exfoliation system via chemical liquid approach. The EDS provided more evidence on elements analysis of atomic MoS_2.

The number of MoS_2 layers can be identified from the edge state as shown in Figure 2(e), there were two layers of exfoliated MoS_2 with the thickness of 1.34 nm. The interplanar spacing of 0.27 nm can be directly measured from the high-resolution TEM image (Figure 2(f)), which was consistent with *d* spacing of hexagonal MoS_2 (100) planes. Moreover, the grain boundaries appeared obviously on the basal surface of exfoliated MoS_2, enlarged by square in red line. It was fundamental to achieve the understanding of edges-dependent magnetic property; there were more high-resolution TEM images of layered MoS_2 in the supporting information S2, expecting to provide a feedback on the morphology of exfoliated MoS_2 layers for the correlated activity.

XRD was carried out as shown in Figure 3(a); the strong diffraction peak (002) revealed the higher crystallinity of exfoliated MoS_2 compared to that of the pristine MoS_2 in bulk. Other minor diffractions, such as (004), (103), (006), (105), (110) and (008) existed obviously, implying the nanoscaled crystallites in different orientations. Furthermore, the full width at half maximum (FWHM) value of the (002) diffraction peak was calculated by using the *Scherrer Equation*, and we estimated the thickness of MoS_2 planes along the *c* axis around 2.1 nm, which was approximately equal to three layers according to the interlayer spacing of 0.63 nm, corresponding to the result of HRTEM measurement.

Further structural characterizations were obtained by Raman spectroscopy with a 532 nm laser excitation. Figure 3(b) demonstrated Raman spectra of exfoliated MoS_2 nanosheets (blank line), the peaks located at 389.4 and 405.9 cm^{-1} were identified as E^1_{2g} and A_{1g} modes, which were associated with vibrations of Mo and S atoms in the basal plane and out-of-plane respectively. The frequency of the E^1_{2g} vibration exhibited red shift, while A_{1g} mode appeared blue shift compared to these of MoS_2 in bulks (E^1_{2g} at 385.1 eV and A_{1g} at 411.3 eV in red line). It indicated that the rate of frequencies for both two modes demonstrated a slight variation with the thickness decreasing of exfoliated MoS_2. For films of more than five layers, the frequencies of both modes converged

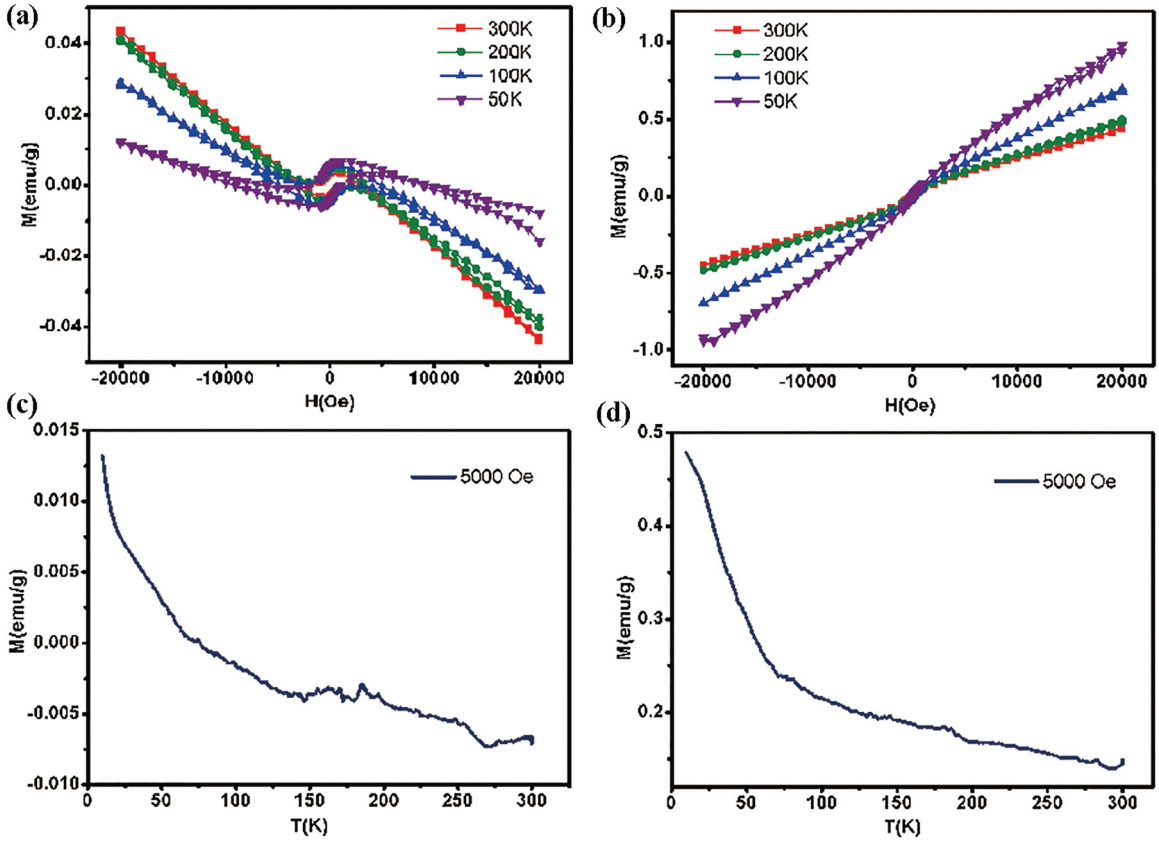

Figure 4. Magnetic evidence for pristine bulk MoS_2 and exfoliated edges-rich structural MoS_2. Magnetization (*M*) vs. applied field (*H*) data taken at different temperatures with field parallel for (a) pure bulk MoS_2 and (b) layered MoS_2 basal planes. (c) Magnetic susceptibility of pristine MoS_2. (d) Magnetic susceptibility of exfoliated MoS_2 nanosheets.

to the bulk values. We evaluated that the numbers of layered MoS_2 were less than three layers according to previous report [39]. In addition, the absorption spectrum of monolayer MoS_2 was plotted to investigate the optical property compared to the pristine bulk MoS_2 without UV-vis absorption. The two principal absorption features at 615 and 678 nm were associated with the A and B excitations of MoS_2 (Figure 3(c)). XPS illustrated characteristic Mo and S peaks respectively, revealing the high purity of ultrathin MoS_2 without any other magnetic impurity as shown in Figure 3(d). In comparison, there was not obvious difference from XPS survey between the exfoliated MoS_2 and bulk MoS_2 except for rather stronger peaks of O and C in pristine MoS_2, which indicated some interaction with air and carbon contamination on the surface of measured sample.

The magnetization (M) vs. temperature (T) measurements were conducted to prove the magnetism of obtained MoS_2 layers in detail. There was an obvious diamagnetic signal shown in Figure 4(a), indicating that the diamagnetism was dominated in bulk MoS_2. However, the clear ferromagnetic parts in exfoliated MoS_2 nanosheets were observed in Figure 4(b), which demonstrated the ferromagnetic function in edges-rich structural MoS_2 nanosheets even though the diamagnetic and paramagnetic background superimposing in some extend. The magnetic susceptibility of pristine MoS_2 and exfoliated MoS_2 nanosheets was plotted respectively as shown in Figure 4(c) and (d). The susceptibilities were determined from the slope of $M(H)$ curves taken at the particular temperatures. There was no long-range magnetic ordering existed in the bulk sample, which illustrated the diamagnetic property. However, the magnetic susceptibility of layered MoS_2 demonstrated typical long-range magnetism, and obviously the magnetization of exfoliated MoS_2 nanosheets was over 10–40 times superior to the bulk MoS_2 comparing with the value of curves.

$M(H)$ curves were magnified magnetization at low field to observe the coercivity dependency in temperature at 10, 100 and 300 K shown in the Figure 5(a)–(c). And it exhibited that the coercive fields were clearly observed in different temperatures, up to 261, 85, 68 Oe respectively, and the coercive field was in decline trend with the temperature increasing, which supplied a strong evidence for the ferromagnetic signal existed in the layered MoS_2. In addition, the zero field cooling (ZFC)/field cooling (FC)

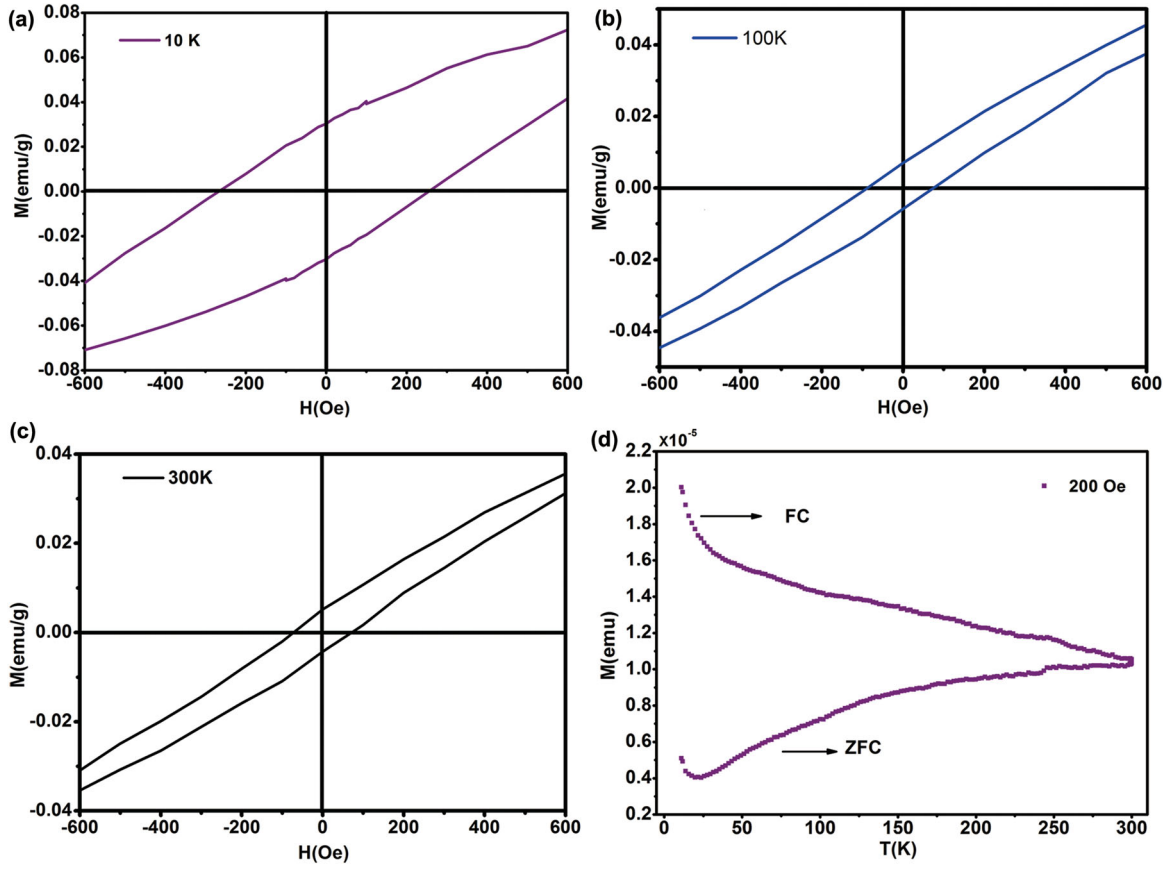

Figure 5. Magnetic evidence for exfoliated edges-rich structural MoS_2. Curves are magnified magnetization at low field to observe the coercivity dependency in temperature at 10, 100 and 300 K of exfoliated MoS_2 nanosheets (a)–(c). (d) The ZFC/FC curves of the layered MoS_2 measured at 5000 Oe.

curves of the layered MoS_2 were measured at 5000 Oe as shown in Figure 5(d). The bifurcation phenomenon between ZFC and FC curves was quite obvious, illustrating the ferromagnetism of layered MoS_2 nanosheets. This particular magnetism phenomenon was possibly triggered due to the exfoliation of MoS_2 with edges structure via chemical liquid. Mostly, this ferromagnetic property was controlled by their inter-atomic distances, and edges structure, furthermore considerable zigzag edge structures located in the grain boundary [35], where the magnetic property was induced. Particularly, the creation of MoS_2 triple vacancy resulted in a significantly magnetic moment in this system [18]. This clearly indicated edge structures or basal plane dislocation during exfoliation using chemical liquid, exhibiting ferromagnetic property in the exfoliated MoS_2 nanosheets, which was consistent with the TEM measurements.

Magnetic force microscopy (MFM) was a typical mode of the noncontact scanning force microscopy, which was an important analytical technique for the near-surface stray-field variation of magnetic materials. It was recognized that the detection of magnetostatic interactions at a local scale was possible by equipping the force microscope with a ferromagnetic probe [40,41]. Firstly, we captured the surface morphology of layered MoS_2 by atomic microscopy force (AMF) as shown in Figure 6(a), the thickness of exfoliated MoS_2 was estimated to about 2.1 nm averagely, three layers of MoS_2 nanosheets approximately (Figure 6(b)). Then MFM image showed that the exfoliated MoS_2 demonstrated a strong magnetic activity (Figure 6(c)).

The absorption force as well as repulsive force appeared during the interaction coupling of the ferromagnetic probe and the stray-field produced by exfoliated MoS_2. As the magnetization directions of probe and sample domain structure were opposite, then the interaction force exhibited attractable which was an absorption force presenting dark contrast in MFM image. On the contrary, Figure 6(c) demonstrated bright contrast, which illustrated the repulsive interaction between the probe and exfoliated MoS_2 sample domain structure. Figure 6(d) showed three-dimensional image of magnetic layered MoS_2; the bright contrast can be observed clearly. However, the magnetic domain structure (especially the edges) could not be captured obviously in the MFM image; it might be caused by factors such as the magneto-crystalline anisotropy and magnetostriction energies. Additionally, lattice defects, stresses and

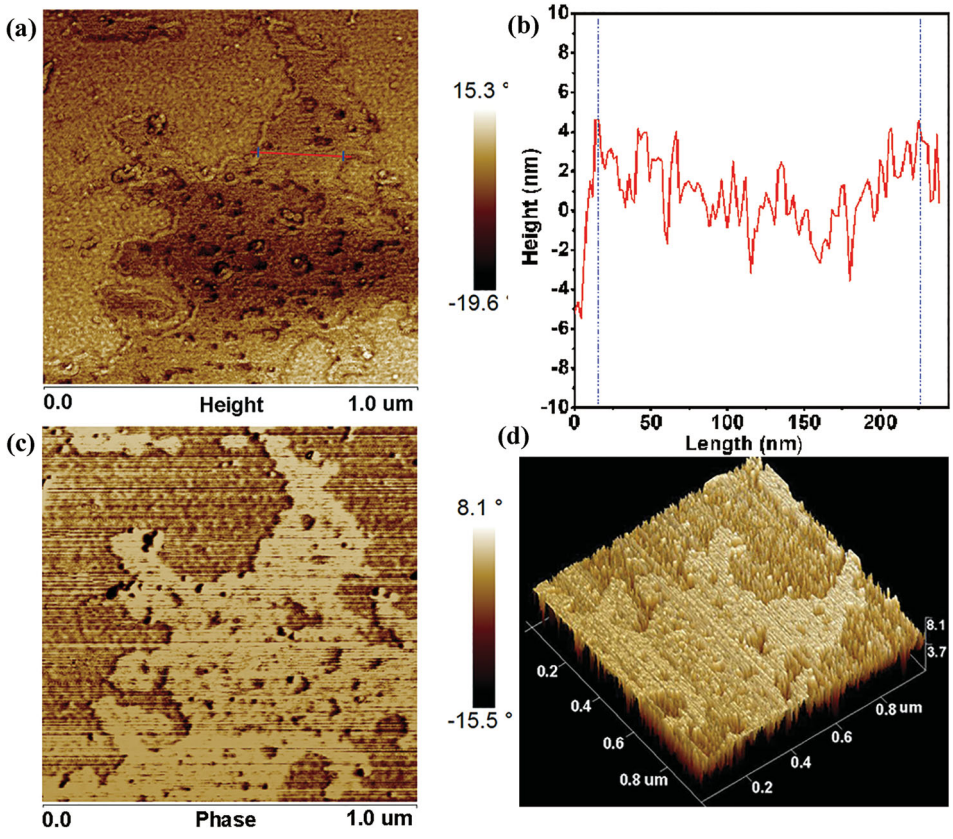

Figure 6. (a) AFM image taken on layered MoS_2 nanosheets tracks of 1.0 μm periodicity. (b) Thickness of the layered MoS_2 nanosheets with red line in image (a). (c) MFM image taken on layered MoS_2 nanosheets tracks of 1.0 μm periodicity, with the lifting the cantilever probe up to 30 nm from the sample surface to measure a long-range interaction. (d) The 3D image of (b).

the surface topology exhibited an additional influence on the domain structure. It was necessary to explore magnetic domain structure in exfoliated MoS_2 nanosheets. Interestingly, there were vacancies exposed crossing the full-scale film in MFM images, the possible reason was that we captured several layered MoS_2 nanosheets in a large scale parallel length of 1 μm, so that the presence of defects including atomic vacancies, displacement can be demonstrated in the MFM condition due to the color variation with the depth of tested film.

Herein, we found that the ferromagnetic performance of exfoliated MoS_2 nanosheets was dependent on the amount of edge sites and size, which played a significant role on triggering typical magnetism. There were plenty of edge sites observed which could provide more localized defects or vacancies promption. Then the spins of the localized defects aligned these of the nearby electron carriers, which produced an effective magnetic field and activated the ferromagnetic performance. Therefore, we addressed the chemical liquid assisted with robust sonication to endow more edge sites or smaller size of exfoliated MoS_2 nanosheets, expecting to be generalized to tune the magnetic properties of other two-dimensional nanosheets.

Conclusion

In summary, a comprehensive analysis focused on the exfoliated edges-rich MoS_2 layers via chemical liquid strategy revealed their intrinsic ferromagnetism. The magnetic measurements illustrated the clear ferromagnetic property of exfoliated MoS_2, in contrast to the pristine MoS_2 in bulks showing diamagnetism. This was attributed to the presence of edges-rich structure on grain boundaries, which was confirmed by the TEM, XPS and MFM investigations. However, the results of MFM images could not capture a strong direct proof on the edges state magnetism due to the resolution of MFM facility; we expected to explore further analysis and to provide reliable evidences which would identify the irregular edge states engineering ferromagnetism. Additionally, the coupling of spin and dislocations might exist during exfoliation with intense sonication, triggering the magnetic property, and it was essential to explore further simulation for ferromagnetic mechanism of exfoliated MoS_2 with zigzag edges structure theoretically.

Acknowledgements

We are appreciated for the contributions from Prof. Angel Rubio and Dr Lede Xian in Universidad del País Vasco/Euskal Herriko Unibertsitatea (UPV/EHU), Spain.

Funding

The presented research was financially supported by the Natural Science Foundation of China (21401211, 81501580, 31571013), the Science and Technology Department of Guangdong Province (2013B010403014), The Project Supported by Guangdong Natural Science Foundation (2016A030312006), Key International Science and Technology Cooperation Project (2015DFH50230), Instrument Developing Project of Chinese Academy of Science (YZ201439), the Science and Technology Program of Shenzhen (KQCX20140521115045447, JCYJ20120615124830232, JCYJ20160429191503002). Additionally, we are appreciated for the contributions from Prof. Angel Rubio and Dr. Lede Xian in Universidad del País Vasco/Euskal Herriko Unibertsitatea (UPV/EHU), Spain.

References

[1] Yu Y, Li C, Liu Y, et al. Controlled scalable synthesis of uniform, high-quality monolayer and few-layer MoS_2 films. Sci Rep. 2013;3(1866):1–6.
[2] Cai L, He J, Liu Q, et al. Vacancy-induced ferromagnetism of MoS_2 nanosheets. J Am Chem Soc. 2015;137:2622–2627.
[3] Yang L, Cui X, Zhang J, et al. Lattice strain effects on the optical properties of MoS_2 nanosheets. Sci Rep. 2014;4(5649):1–7.
[4] Wang QH, Kalantar-Zadeh K, Kis A, et al. Electronics and optoelectronics of two-dimensional transition metal dichalcogenides. Nat Nanotechnol. 2012;7:699–712.
[5] Jaramillo TF, Jorgensen KP, Bonde J, et al. Identification of active edge sites for electrochemical H_2 evolution from MoS_2 nanocatalysts. Science. 2007;317:100–102.
[6] Huang X, Zeng Z, Zhang H. Metal dichalcogenide nanosheets: preparation, properties and applications. Chem Soc Rev. 2013;42:1934–1946.
[7] Li H, Wu J, Yin Z, et al. Preparation and applications of mechanically exfoliated single-layer and multilayer MoS_2 and WSe_2 nanosheets. Acc Chem Res. 2014;47:1067–1075.
[8] Huang X, Tan C, Yin Z, et al. 25th Anniversary article: Hybrid nanostructures based on two-dimensional nanomaterials. Adv Mater. 2014;26:2185–2204.
[9] Najmaei S, Zou X, Er D, et al. Tailoring the physical properties of molybdenum disulfide monolayers by control of interfacial chemistry. Nano Lett. 2014;14:1354–1361.
[10] Najmaei S, Liu Z, Zhou W, et al. Vapour phase growth and grain boundary structure of molybdenum disulphide atomic layers. Nat Mater. 2013;12:754–759.
[11] Huang X, Zeng Z, Bao S, et al. Solution-phase epitaxial growth of noble metal nanostructures on dispersible single-layer molybdenum disulfide nanosheets. Nat Commun. 2013;4:1444–1452.
[12] Chen J, Wu X, Yin L, et al. One-pot synthesis of CdS nanocrystals hybridized with single-layer transition-metal dichalcogenide nanosheets for efficient photocatalytic hydrogen evolution. Angew Chem Int Ed. 2015;54:1210–1214.
[13] Liu J, Zeng Z, Cao X, et al. Preparation of MoS_2-polyvinylpyrrolidone nanocomposites for flexible nonvolatile rewritable memory devices with reduced graphene oxide electrodes. Small. 2012;8:3517–3522.

[14] Yin Z, Li H, Jiang L, et al. Single-layer MoS_2 phototransistors. ACS Nano. 2012;6:74–80.
[15] Yin Z, Chen B, Bosman M, et al. Au nanoparticle-modified MoS_2 nanosheet-based photoelectrochemical cells for water splitting. Small. 2014;10:3537–3543.
[16] Ramakrishna Matte HSS, Gomathi A, Manna AK, et al. MoS_2 and WS_2 analogues of graphene. Angew Chem Int Ed. 2010;49:4059–4062.
[17] Chou SS, De M, Kim J, et al. Ligand conjugation of chemically exfoliated MoS_2. J Am Chem Soc. 2013;135:4584–4587.
[18] Hao G, Huang Z, Liu Y, et al. Electrostatic properties of few-layer MoS_2 films. AIP Adv. 2013;3:1–6.
[19] Hao G, Fan Y, Qi X, et al. Growth, characterization of epitaxial heterostructures of ultrathin Bi_2Te_3 nanoplates on few-layer MoS_2 films. Sci Adv Mater. 2014;6:383–386.
[20] Pan J, Du S, Zhang Y, et al. Ferromagnetism and perfect spin filtering in transition-metal-doped graphyne nanoribbons. Phys Rev B. 2015;92:1–6.
[21] Pereira VM, Castro Neto AH. Strain engineering of graphene's electronic structure. Phys Rev Lett. 2009;103:1–4.
[22] Pan H, Zhang YW. Tuning the electronic and magnetic properties of MoS2 nanoribbons by strain engineering. J Phys Chem C. 2012;116:11752–11757.
[23] Zhang J, Soon JM, Loh KP, et al. Magnetic molybdenum disulfide nanosheet films. Nano Lett. 2007;7:2370–2376.
[24] He J, Wu K, Sa R, et al. Magnetic properties of nonmetal atoms absorbed MoS_2 monolayers. Appl Phys Lett. 2010;96:1–3.
[25] Botello-Méndez AR, López-Urías F, Terrones M, et al. Metallic and ferromagnetic edges in molybdenum disulfide nanoribbons. Nanotechnology. 2009;20:1–9.
[26] Wang ZY, Li H, Liu Z, et al. Mixed low-dimensional nanomaterial: 2D ultranarrow MoS_2 inorganic nanoribbons encapsulated in quasi-1D carbon nanotubes. J Am Chem Soc. 2010;132:13840–13847.
[27] Li YF, Zhou Z, Zhang SB, et al. MoS_2 nanoribbons: high stability and unusual electronic and magnetic properties. J Am Chem Soc. 2008;130:16739–16744.
[28] Ataca C, Sahin H, Aktürk E, et al. Mechanical and electronic properties of MoS_2 nanoribbons and their defects. J Phys Chem C. 2011;115:3934–3941.
[29] Pan H, Zhang YW. Edge-dependent structural, electronic and magnetic properties of MoS_2 nanoribbons. J Mater Chem. 2012;22:7280–7290.
[30] Hod O, Barone V, Peralta J, et al. Enhanced half-metallicity in edge-oxidized zigzag graphene nanoribbons. Nano Lett. 2007;7:2295–2299.
[31] Zheng HP, Yang BS, Wang DD, et al. Tuning magnetism of monolayer MoS_2 by doping vacancy and applying strain. Appl Phys Lett. 2014;104:132403–132405.
[32] Dutta S, Manna A, Pati SK. Intrinsic half-metallicity in modified graphene nanoribbons. Phys Rev Lett. 2009;102:1–4.
[33] Kan EJ, Li Z, Yang JL, et al. Half-metallicity in edge-modified zigzag graphene nanoribbons. J Am Chem Soc. 2008;130:4224–4225.
[34] Son YW, Cohen ML, Louie SD. Half-metallic graphene nanoribbons. Nature. 2006;444:347–349.
[35] Chen L, Guo L, Li Z, et al. Towards intrinsic magnetism of graphene sheets with irregular zigzag edges. Sci Rep. 2013;3:1–6.
[36] Gao DQ, Si MS, Li JY, et al. Ferromagnetism in freestanding MoS_2 nanosheets. Nanoscale Res Lett. 2013;8:129–137.
[37] Han SW, Hwang YH, Kim SH, et al. Controlling ferromagnetic easy axis in a layered MoS_2 single crystal. Phys Rev Lett. 2013;110:1–5.
[38] Gao GH, Gao W, Cannuccia E, et al. Artificially stacked atomic layers: toward new van der waals solids. Nano Lett. 2012;12:3518–3525.
[39] Lee C, Yan H, Brus LE, et al. Anomalous lattice vibrations of single- and few-layer MoS_2. ACS Nano. 2010;4:2695–2700.
[40] Hartmann U. Magnetic force microscopy. Annu Rev Mater Sci. 1999;29:53–87.
[41] Li H, Qi X, Wu J, et al. Investigation of MoS_2 and graphene nanosheets by magnetic force Microscopy. ACS Nano. 2013;7:2842–2849.